*Proc. Natl. Acad. Sci. USA*
Vol. 96, pp. 2048–2053, March 1999
Biophysics

# Protrusive growth from giant liposomes driven by actin polymerization

HIDETAKE MIYATA*†‡, SHUJI NISHIYAMA*, KEN-ICHIROU AKASHI*, AND KAZUHIKO KINOSITA, JR.§

*Department of Physics, Faculty of Science and Technology, Keio University. 3-14-1 Hiyoshi, Kohoku-ku, Yokohama 223-8522, Japan; and §Core Research for Evolutional Science and Technology (CREST) "Genetic Programming" Team 13, Nogawa 907, Miyamae-ku, Kawasaki 261-0001, Japan

*Edited by Shinya Inoue, Marine Biological Laboratory, Woods Hole, MA, and approved December 30, 1998 (received for review August 10, 1998)*

**ABSTRACT** **Development of protrusions in the cell is indispensable in the process of cell motility. Membrane protrusion has long been suggested to occur as a result of actin polymerization immediately beneath the cell membrane at the leading edge, but elucidation of the mechanism is insufficient because of the complexity of the cell. To study the mechanism, we prepared giant liposomes containing monomeric actin (100 or 200 $\mu$M) and introduced KCl into individual liposomes by an electroporation technique. On the electroporation, the giant liposomes deformed. Most importantly, protrusive structure grew from the liposomes containing 200 $\mu$M actin at rates (ranging from 0.3 to 0.7 $\mu$m/s) similar to those obtained in the cell. The deformation occurred in a time range (30 ~ 100 s) similar to that of actin polymerization monitored in a cuvette (*ca*. 50 s). Concomitant with deformation, Brownian motion of micron-sized particles entrapped in the liposomes almost ceased. From these observations, we conclude that actin polymerization in the liposomes caused the protrusive formation.**

Actin is one of the most important components of intracellular structures such as stress fibers or cell cortex. With the aid of a variety of actin-binding proteins and regulatory proteins, it can undergo a cycle of polymerization and depolymerization, thereby participating in protrusive activities that occur at the leading edge of the cell (1–7). Polymerization of actin, hence the elongation of actin filaments immediately beneath the cell membrane, is assumed to be the origin of the protrusive force: the elongating actin filament is supposed to "push out" the cell membrane. This possibility has been discussed from the viewpoint of energetics (8, 9). Recently, a mechanistic model has been proposed (10, 11). However, whether cells actually use this mechanism or how this mechanism is realized in the cell remains totally unclear.

To elucidate the role of actin polymerization in the protrusive phenomena, several groups have developed model systems, i.e., liposomes containing purified actin monomers (12–17). In this approach, the actin-containing liposome is regarded as a reconstructed *in vitro* cell model that provides a unique opportunity to study mechanochemical aspects of the actin filament growth. In these model systems, polymerization of actin encapsulated in liposomes and accompanying shape changes have been achieved by introducing mono- or divalent cations by using ionophores into the liposomes (12–16) or by raising temperatures in the presence of submillimolar $Ca^{2+}$ ions that had been encapsulated in the liposomes along with actin monomers (17). However, in most cases except for one (13), liposomes did not develop protrusive structure and assumed irregular or elongated shape. In contrast with this, thin and rigid protrusive structure grew from the liposomes containing tubulin (18). The fact that actin filament is far less rigid than a microtubule (19, 20) may imply that it is a passive structural unit supporting, rather than generating, such structure as protrusion. Nevertheless, because it is actin that localizes at the leading edge of the cell and plays a dynamic as well as a structural role (21), it is highly likely that actin is an active mechanochemical component. Hence, studying the mechanochemical aspect of the actin polymerization by using the reconstituted system is absolutely necessary.

We applied the electroporation technique to introduce KCl into actin-containing liposomes. With this method, we could initiate at a desired instance actin polymerization in a selected liposome at an ionic strength much higher than we previously used, and we could continuously observe liposome shape change. In particular, we have succeeded in observing protrusive growth from the liposomes at rates comparable to those observed in highly motile cells.

## MATERIALS AND METHODS

**Materials.** Actin was purified from rabbit skeletal muscle acetone powder (22) and further purified over a G-150 Sephadex column (23). A potassium ion indicator dye, PBFI, and rhodamine maleimide were obtained from Molecular Probes. Dimyristoylphosphatidylcholine and cardiolipin (from bovine heart, Na salt) were purchased from Avanti Polar-Lipids. All other chemicals were of analytical grade. Rhodamine-labeled actin was prepared by incubating G-actin with equimolar amount of rhodamine maleimide at 0°C for 90 min, followed by termination of the reaction with 2 mM DTT. The reactant was dialyzed against 200 ml G buffer (2 mM tris(hydroxymethyl)aminomethane (pH 8.0)/0.2 mM $CaCl_2$/0.2 mM ATP/0.2 mM $NaN_3$/5 mM 2-mercaptoethanol) for 18 h with one change of the buffer, and the dialyzed material was passed through the G-150 column to obtain purified rhodamine-labeled G-actin. A mixture of crosslinked actin oligomers was prepared by crosslinking F-actin with p-phenylenedimaleimide according to the method of Knight and Offer (24). After the crosslinking reaction, the crosslinked actin was dialyzed against G-buffer followed by ultracentrifugation at $3.5 \times 10^5 \times g$ for 30 min. The supernatant was collected and was used in the experiment without further purification. Analysis with SDS/PAGE revealed that the supernatant fraction contained actin monomers, dimers and trimers. No attempt was made to separate the three components. We hereafter call this supernatant nuclei mixture for convenience.

**Preparation of Actin-Containing Liposomes.** Actin-containing liposomes were prepared by swelling at 0°C of the dried lipid film (prepared from the mixture of 150 $\mu$g dimyristoylphosphatidylcholine and 150 $\mu$g cardiolipin) in 50 $\mu$l internal solution (G-buffer plus 0.1 M sucrose and 0.4 mg/ml BSA) containing G-actin (200 $\mu$M or 100 $\mu$M) and, when

The publication costs of this article were defrayed in part by page charge payment. This article must therefore be hereby marked "*advertisement*" in accordance with 18 U.S.C. §1734 solely to indicate this fact.

PNAS is available online at www.pnas.org.

This paper was submitted directly (Track II) to the *Proceedings* office.
†Present address: Physics Department, Graduate School of Science, Tohoku University, Aramaki, Aoba-ku, Sendai 980-8578, Japan.
‡To whom reprint requests should be addressed. e-mail: miyata@bio.phys.tohoku.ac.jp.

necessary, the nuclei mixture at an appropriate concentration. After the swelling, 1 $\mu$l of the concentrated liposome solution was mixed with 500 $\mu$l G-buffer supplemented with 0.1 M glucose in an observation chamber that was made from silicone rubber sheet (3 mm thick) stuck onto a 24 × 36 mm coverslip without adhesive (25). To this mixture was added 500 $\mu$l G-buffer supplemented with 60 mM KCl: the final ionic condition of the medium surrounding the liposomes (external solution) was 2 mM tris(hydroxymethyl)aminomethane (pH 8.0)/0.2 mM $CaCl_2$/0.2 mM ATP/0.2 mM $NaN_3$/50 mM glucose/30 mM KCl/0.2 mg/ml BSA. The concentration of actin and the nuclei mixture outside the liposomes was 1/1,000 of the initial concentration, and the polymerization of actin outside the liposomes should be negligible.

**Observation of Liposomes.** Observation of the actin-containing liposomes was carried out on an inverted microscope (ICM405, Zeiss) equipped with a 100×, oil-immersion objective (numerical aperture = 1.3) either in phase contrast or epifluorescence mode. A charge-coupled-device camera (C3077, Hamamatsu, Ichinocho, Japan) was used to acquire phase contrast images, and a silicon-intensified target camera (C-1000, Hamamatsu) was used to acquire epifluorescence images. Images of the liposome were recorded on S-VHS or Hi8 video tapes for later analysis. We characterized the liposomal shape on the basis of their cross-sectional views, because the liposomes settling on the bottom of the observation chamber because of higher density of the internal solution could not be viewed from the side.

**Electroporation of Liposomes.** Electroporation was carried out according to the method of Hibino *et al.* (26) with slight modifications. As depicted in Fig. 1 *Upper*, a pair of electrodes made from a platinum wire (diameter = 0.3 mm) was fixed on a pair of Plexiglas rods that were attached to micromanipulators. The center-to-center distance of the electrodes was adjusted between 0.9 and 1.1 mm. In each experiment a liposome having a diameter of 8–18 $\mu$m was selected by phase contrast microscopy and was placed in the middle of the electrode pair.

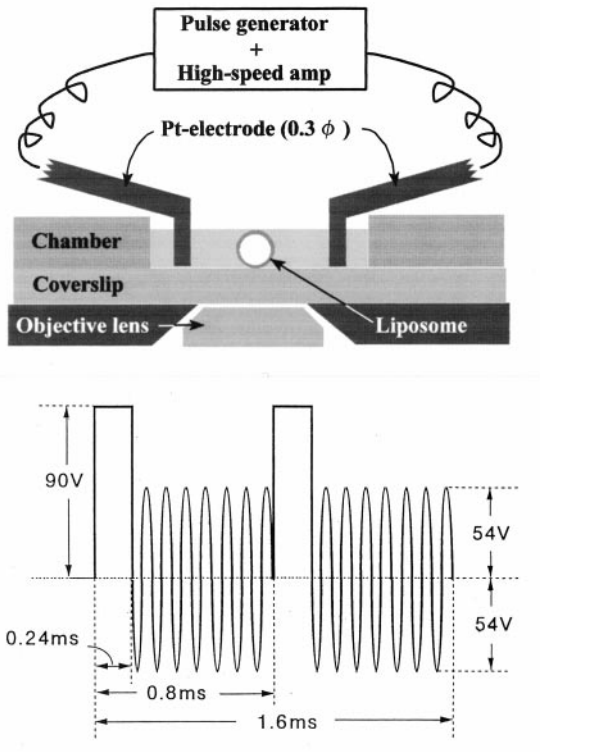


FIG. 1. (*Upper*) A schematic representation of the electroporation setup. Observations were made in an open chamber. A liposome was placed in the middle of a pair of Pt wire electrodes that were fixed on Plexiglas rods (not shown) for adjustment of the position of the electrodes. (*Lower*) A shape of the electric pulse used for electroporation.

An electric pulse as depicted in Fig. 1 *Lower* was synthesized with a function generator (Model 395, Wavetek, San Diego), amplified with a high-speed power amplifier (Model 4015, NF Electronics Instruments, Tokyo) and then was applied to the selected liposomes. We attempted to use a single rectangular pulse (100 V, 1.2 ms duration), but the shape change did not occur (S.N. and K-i.A., unpublished observations). Because the sizes of the selected liposomes were sufficiently small compared with the separation and the diameter of the electrode, the electric field around the liposome could be regarded as uniform. The magnitude of the membrane potential, $\phi$, across the liposomal membrane facing the electrodes, is thus calculated to be $\phi = 3aV/\{d \times \ln(d/r-1)\}$, where $a$ is the radius of the liposome, $V$ the applied voltage, $d$ the separation, and $r$ the radius of the electrode. The calculated membrane potential was 1–1.8 V. Reported membrane potential causing poration of cell membranes is ≈1 V (27).

By encapsulating a potassium ion indicator, PBFI (28), in the liposomes and monitoring the increase of its fluorescence, we confirmed that KCl entered the liposomes within 1 sec after the application of the electric pulse. The PBFI fluorescence did not always increase on the pulse application, presumably because some of the encapsulated PBFI leaked on the electroporation: we observed a fluorescent cloud of PBFI around the liposome surface facing the negative electrode (S.N. and K-i.A., unpublished observations). It has been suggested that lipid membranes become permeable to low molecular weight substances when a strong electric field is applied to the membranes (29).

**Monitoring Actin Polymerization in Liposomes.** To monitor actin polymerization in the liposomes, Brownian motion of small particles (1 $\mu$m polystyrene beads that were added to the internal solution or small lipid aggregates of similar size that were entrapped in the liposomes during the liposome preparation) were observed. If actin polymerizes, Brownian motion of these particles will almost stop, because the particle diameter exceeds the size of the mesh of the actin filament network (30). Polystyrene beads (carboxylated, Polysciences) were washed several times in the internal solution and were added to the internal solution at a concentration of 0.2% (wt/vol). Results with liposomes apparently containing no small particle or those containing particles too small to be clearly observed were not analyzed, although shape change occurred in those liposomes (not shown).

**Measurement of Protrusion Length.** Video sequences containing clear images of liposomes were selected, and each sequence was processed with an image processor (Argus 20, Hamamatsu) for removal of mottles, background subtraction, and contrast enhancement. Images averaged over four frames were fed to a Macintosh computer (Power Mac, 8500/180) for image capturing and analysis with the public-domain National Institutes of Health IMAGE program (developed at the National Institutes of Health and available from the Internet by anonymous file transfer protocol from zippy.nimh.nih.gov or on floppy disk from the National Information Service; part number PB95-500195GEI.) For presentation of the process of liposome deformation, appropriate images were intermittently captured. When the protrusion growth was analyzed, the images were captured every 1 s after the application of the electric pulse. To quantify the development of protrusions, distance was measured between the tip of the protrusion and a reference point arbitrarily fixed in the liposome, as indicated with the symbol × in Fig. 2*d*. From the video sequence, we judged the appearance of protrusions by eye, and the time of the start of the elongation was determined accordingly. Change in the distance between the reference point and the tip

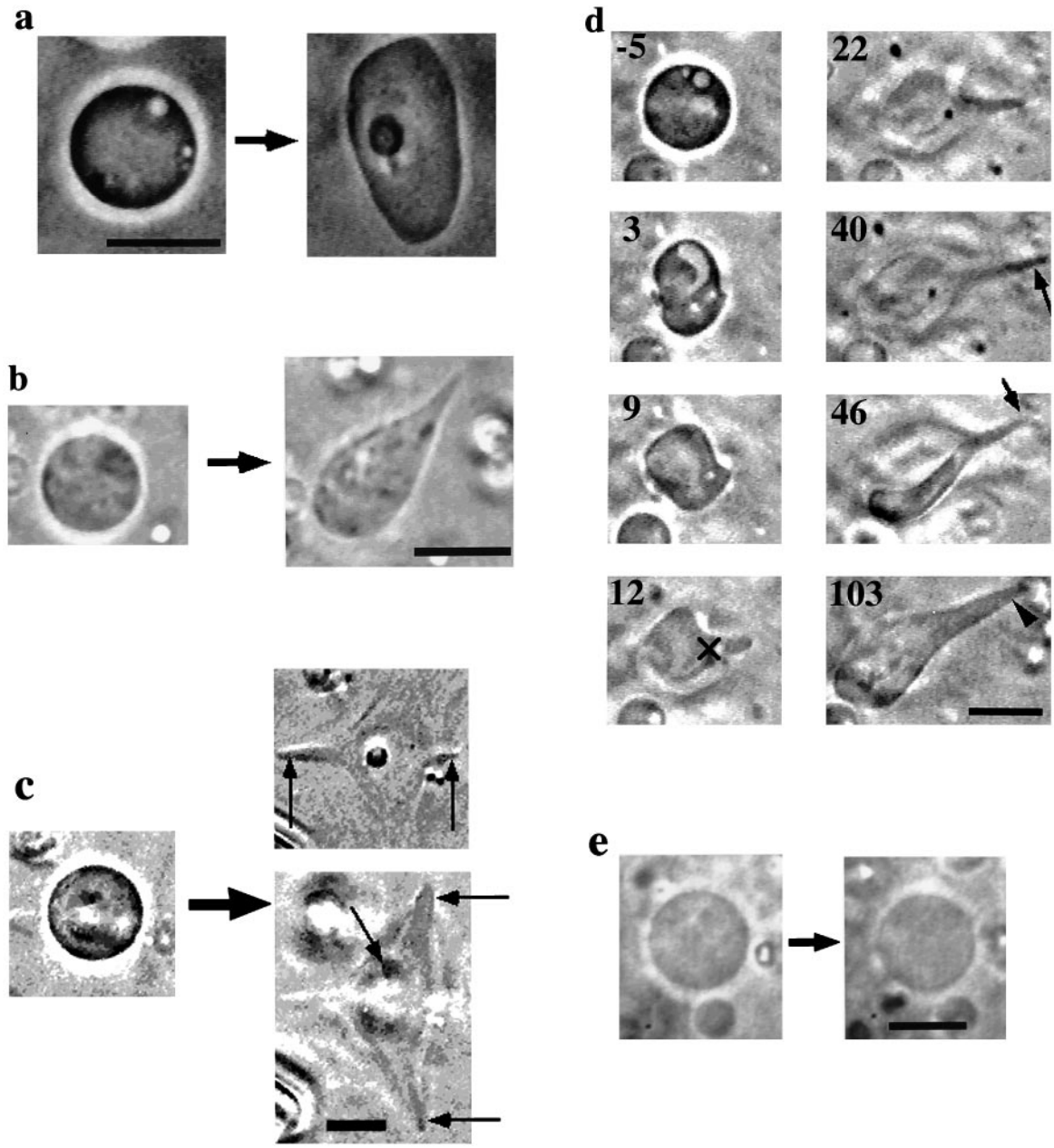


FIG. 2. (*a–d*) Phase-contrast micrographs of the liposomes containing actin observed after the electroporation. (*a*) A liposome transforming into an irregular shape; (*b* and *c*) Liposomes developing protrusions. In *c*, the liposome was found to develop five protrusions lying at different focus levels, as indicated with arrows in the panels (*Upper Right*, lower focus; *Lower Right*, higher focus). We could record the development of only two of them, indicated with vertical arrows. (*d*) Process of protrusive growth. Number in each frame represents the time in sec elapsed after the pulse application. The symbol × indicates the reference point used to determine the rate of protrusive formation (see text). (*e*) Comparison of the shape of a liposome containing 100 $\mu$M BSA before and after the electroporation. Bars, 10 $\mu$m.

was plotted and was presented as a time course of the protrusive elongation.

## RESULTS

**Classification of the Shape of Liposomes After the Pulse Application.** After the application of the electric pulse, approximately one-half to one-third of the challenged actin-containing liposomes changed their shape, as summarized in Table 1. The resultant shapes were classified into three types on the basis of their cross-sectional view: undeformed, irregular (see Fig. 2*a*) and protrusive shape (the shape with protrusions; Fig. 2 *b–d*). Table 1 shows that more than half of the liposomes containing 200 $\mu$M actin plus 10 $\mu$M nuclei mixture changed their shape. Similar morphologies were observed for the liposomes containing 200 $\mu$M actin plus 2 $\mu$M nuclei mixture or 200 $\mu$M actin alone. About one-third of the liposomes containing 100 $\mu$M actin and 10 $\mu$M nuclei mixture assumed irregular shape, but no protrusive shape was observed. Without actin, no deformation occurred (Fig. 2*e*). Some of the deformed liposomes eventually regained approximately circular shape (Table 1; see below), but we regarded these as deformed.

The protrusions possessed a variety of sizes and shapes, as shown in Fig. 2 *b–d*. Some liposomes developed several protrusions in various directions (Fig. 2*c*). Correlation between the direction of the protrusive growth and that of the electric field was not clear, because rotation of liposomes could have occurred immediately after the pulse application. Despite their large axial ratio, the protrusions were considerably rigid:

Table 1. Summary of liposome deformation

| Conditions | | Type of deformation | | | |
|---|---|---|---|---|---|
| Actin, $\mu$M | Nuclei, $\mu$M | Irregular | Protrusive | Undeformed | Total |
| 200 | 10 | 16[a] | 6 | 17(8) | 39 |
| 200 | 2 | 9[b] | 3[d] | 14(3) | 26 |
| 200 | 0 | 7 | 2[e] | 13(4) | 22 |
| 100 | 10 | 8[c] | 0 | 14(3) | 22 |

*a*, *b*, and *c*, two liposomes in each group regained more or less circular shape after the shape change completed; *d*, one and *e*, two of these liposomes eventually returned to more or less circular shape. For details, see text. Numbers in parentheses, number of liposomes in which Brownian motion of small particles stopped; within all the deformed liposomes (irregular and protrusive), Brownian motion of the small particles stopped.

fluctuation of the shape, such as bending, was small compared with that of long sausage-like liposomes having similar dimensions. These rigid characteristics were quite similar to that of the dumbbell-shaped liposomes containing polymerized actin (17).

**Process of the Protrusive Growth.** Fig. 2*d* shows an example of the process of the protrusive growth. Immediately after pulse application, the liposome greatly deformed, perhaps because of electrodynamic stress (31). Between the moment of the pulse application and the onset of the deformation, there was a time period during which fluctuation of the liposomal membrane became noticeable. In this particular liposome, the fluctuation ceased by about 10 s after the pulse application and the protrusive growth started. It continued until about 40 s. This liposome developed two protrusions that became evident only after changing the focus (indicated with a long arrow at 40 s and with a short arrow at 46 s). But after that, the two protrusions coalesced to form a thicker protrusion (indicated with an arrowhead at 103 s). The detail of the coalescing process was not clear because the two protrusions were lying at different focus levels. Close inspection of the video sequence indicated that inside the liposome, Brownian motion of the small particles became suppressed as the membrane fluctuation became smaller. The reduction of both the Brownian motion of the particles and membrane fluctuation strongly indicates polymerization of the encapsulated actin and hence, the shape change occurred as a consequence of actin polymerization (see below).

**The Temporary Fluctuation of the Liposome Membrane and the Cessation of the Brownian Motion of the Small Particles in the Liposomes.** The temporary fluctuation of the membrane occurred in many, but not all, of the deformed liposomes (both irregular and protrusive shapes) and continued for a few seconds to a few tens of seconds. The membrane fluctuation perhaps arose from the loss of the liposome content, i.e., an increase of the surface-to-volume ratio that occurs on the electroporation. It has been shown that with a given curvature elasticity, a liposome can assume various shapes depending on its surface-to-volume ratios (32).

The cessation of the Brownian motion of small particles occurred 30 $\approx$100 s after the pulse application; the time required for this cessation was difficult to assess, because Brownian motion of the liposomes themselves overlapped. The duration of the deformation was about 30 s from the time point when the shape change became apparent in the video sequences. The membrane fluctuation also occurred in the undeformed liposomes, but the cessation of the Brownian motion of small particles occurred only in part of these liposomes (their numbers are shown in parentheses in Table 1); perhaps inside the undeformed liposomes, which contained moving particles, actin polymerization was not sufficient or did not occur at all.

The percentage of the deformed liposomes containing 200 $\mu$M actin increased with increasing concentration of nuclei mixture (from 40 to 56%; Table 1). Some protrusions grown from the liposomes containing 2 or 0 $\mu$M nuclei mixture disappeared and the liposomes regained nearly circular shape (Table 1); the protrusion, before being lost, wound around the liposome and was absorbed into the liposome body (not shown). A small number of the liposomes assuming the irregular shape also returned to the circular shape (Table 1). In both cases, the motion of small particles remained suppressed, and hence, the change cannot be caused by total depolymerization of actin. At present, the mechanism of these phenomena is not clear; the nuclei mixture may help stabilize the putative actin structures (see *Discussion*), supporting the anisotropic liposome shape, and the structure might become somewhat unstable at lower concentrations of nuclei mixture. This notion is a subject of future study.

**Shape Change of the Liposomes Containing Rhodamine-Labeled Actin.** We observed the shape change of the liposomes containing rhodamine-labeled actin. Fig. 3 is a series of epifluorescence micrographs of a liposome containing the labeled actin. After the pulse application, two protrusive structures appeared at the top and the bottom of the liposome (two arrowheads in the image at 27 s); only the bottom one could be brought into focus. The elongation of the lower protrusion continued until about 40 s. From the comparison of the phase and fluorescence images obtained after the shape change ceased (not shown), we concluded that the whole interior of the liposome was filled with actin. Because the

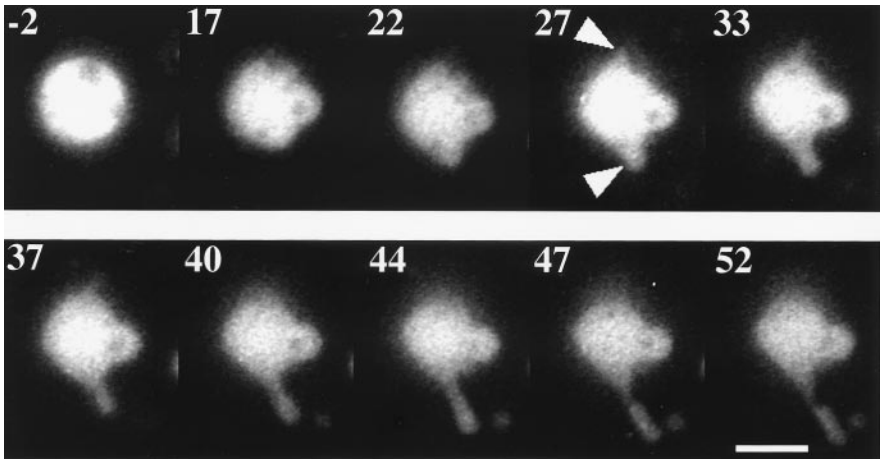


FIG. 3. Shape change of a liposome containing 200 $\mu$M rhodamine-labeled actin and 10 $\mu$M nuclei mixture. Number in each frame represents the time in sec elapsed after the pulse application. Arrowheads, two protrusions. Bar, 10 $\mu$m.

mode of the observation could not be changed quickly enough, the phase images were not available during the period of the shape change. But we presume that actin also filled the liposome interior during the period of the shape change. It is highly unlikely that the empty membrane protrusions first formed, and then actin filled and polymerized in the protrusion.

**Time Course of the Protrusive Growth.** Fig. 4 shows the time course of the elongation of four protrusions measured for three liposomes shown in Fig. 2 *b–d*. The growth rates were determined from the slope of the initial portion of the growth curves. Individual protrusions grew at relatively uniform rates that ranged over 0.34 and 0.71 $\mu$m/s with an average of 0.47 $\mu$m/s. When several protrusions developed from one liposome, we attempted to obtain the time course of as many protrusions as possible; however, because not all the protrusions were lying in the same focal plane, maximally only two protrusions (indicated with vertical arrows in Fig. 2*c*) could be observed simultaneously (represented with symbols ○ and ● in Fig. 4). Decreasing the concentration of the nuclei mixture had no marked effect on the growth rate: the rates that could be measured in the absence of the nuclei mixture were 0.56 and 0.66 $\mu$m/s. The shape change of the liposomes as shown in Fig. 2*a* occurred in 30 to 60 s. Decrease in actin concentration to 100 $\mu$M resulted in longer duration of the shape change (100 to 200 s).

To estimate the duration of actin polymerization, we monitored polymerization of 200 $\mu$M pyrene-labeled actin in a cuvette at 23°C under the same ionic condition as the external solution. The pyrene fluorescence increased and reached 90% of a saturation level at about 50 s after the addition of 30 mM KCl to the cuvette containing actin solution (not shown).

## DISCUSSION

By applying the electroporation technique, we succeeded in controlling the actin polymerization in individual liposomes, thereby continuously observing the shape change from its early stage. On the basis of the observations described above, we suggest that the protrusive growth was driven by actin polymerization. One might argue that the protrusion was generated by a mechanism similar to the formation of a tether, a thin lipid membrane tube that can be pulled out from a red blood cell membrane placed in a flow (33): the tip of the tether was adhered to the substrate. However, in our case the tips of the protrusions were not fixed: the protrusions freely and randomly changed their orientation (about 23 degrees and 17 degrees for the liposomes shown in Fig. 2 *b* and *d*, respectively). Hence, the possibility of the tether formation is excluded. Another phenomenon, the spontaneous transformation, cannot explain our result, because it occurs in a time scale of the order of a few sec (ref. 34; H.M., unpublished observation), which is much shorter than that obtained in our experiment.

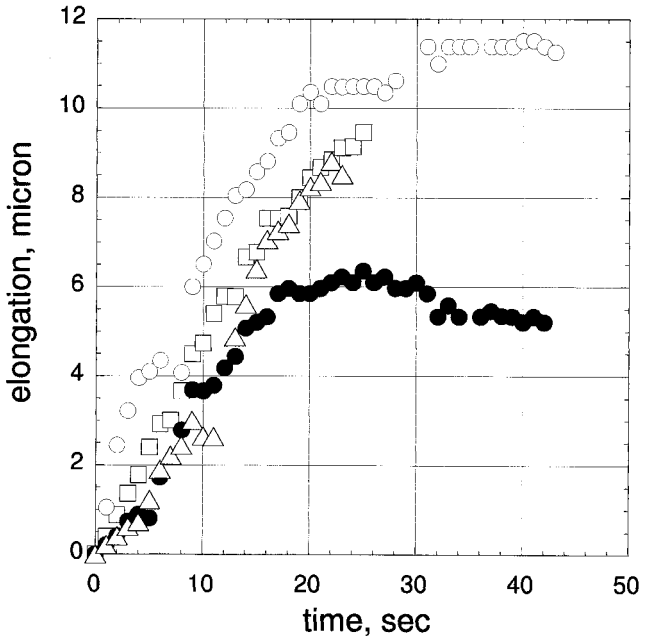


FIG. 4. Time course of the protrusion elongation. The data were obtained from the measurement made for the liposomes shown in Fig. 2 *b–d*. Symbols △ and □ represent the protrusions in *b* and *c*; ○ and ●, the left and right protrusions in *d*. Zero corresponds to the time when protrusion became recognizable by eye.

The reduced fluctuation of the shape of the deformed liposomes implies an existence of rigid structures, such as a bundle or a gel of actin filaments, which would serve as a lining of the otherwise flexible membrane structure (35). It has been shown that if sufficiently high concentrations of actin (above 50 $\mu$M) polymerize, a liquid crystalline phase of actin filaments appears (36). The bundle structures occurred in the liposomes containing 100 $\mu$M actin that had been polymerized with 0.5 mM $CaCl_2$ (17). Thus, it is likely that bundle structures existed within the protrusions; exactly how these actin filaments aligned in the liposomes remains to be determined.

We found that the protrusions grew at rates (average = 0.47 $\mu$m/s), similar to the rate of formation of protrusive structures of the cell: the values obtained here are comparable to the rate of anterior pseudopod extension measured for *Dictyostelium* (0.36 $\mu$m/s; ref. 37), or the rate of lamellar protrusion of polymorphonuclear leukocytes (0.16 $\mu$m/s; ref. 38). The rate of pseudopod extension has been considered to be fairly high, and whether actin polymerization in the cell can support this speed has remained elusive. Our results indicate that the polymerization of actin can drive the protrusive process in the cell. Our study also demonstrated that the protrusive formation did not require any actin-bundling proteins. In the cell, protrusive structures such as microvilli seem to be stabilized by the presence of actin-bundling proteins (39). The role of those proteins in the cell may be to endow mechanical strength to the assemblage of actin filaments and hence to facilitate the protrusive growth.

Recent studies on the molecular mechanism of the protrusive activity has brought into focus the mode of regulation of the protrusive process, such as nucleation of actin polymerization or signaling processes that may control the activity (40–42). The study on the temporal and spatial regulation of actin polymerization at the leading edge will certainly advance our understanding of the molecular mechanism of cell locomotion, but the scenario still lacks the explanation, based on experiments, of how the driving force itself is generated. Our previous study demonstrated that actin polymerization was capable of altering the liposome morphology; however, the rate of the polymerization and hence the shape change were quite low, and the morphology of the liposomes (dumbbell- or disk-shape) was quite different from that of cellular structures (lamellae or protrusion). With the present system, a much higher rate of polymerization and shape change was achieved, and the protrusive structures appeared. The study with the model system may provide a clue to the mechanism of force generation in the protrusive phenomena at the leading edge of the cell.

This work was supported by a grant from the Takeda Science Foundation, a grant from Keio University, and Grants-In-Aid from the Ministry of Education, Science, Sports and Culture of Japan.

1. Condeelis, J. (1993) *Annu. Rev. Cell Biol.* **9,** 411–444.
2. Lee, J., Ishihara, A. & Jacobson, K. (1993) *Trends Cell Biol.* **3,** 366–370.

3. Stossel, T. P. (1993) *Science* **260,** 1086–1094.
4. Grębecki, A. (1994) *Int. Rev. Cytol.* **148,** 37–80.
5. Janmey, P. A. (1994) *Annu. Rev. Physiol.* **56,** 169–191.
6. Zigmond, S. H. (1996) *Curr. Opin. Cell Biol.* **8,** 66–73.
7. Mitchson, T. J. & Cramer, L. P. (1996) *Cell* **84,** 371–379.
8. Hill, T. L. (1981) *Proc. Natl. Acad. Sci. USA* **78,** 5613–5617.
9. Hill, T. L. & Kirschner, M. W. (1982) *Proc. Natl. Acad. Sci. USA* **79,** 490–494.
10. Peskin, C. S., Odell, G. M. & Oster, G. F. (1993) *Biophys. J.* **65,** 316–324.
11. Mogliner, A. & Oster, G. (1996) *Biophys. J.* **71,** 3030–3045.
12. Cortese, J. D., Schwab III, B., Frieden, C. & Elson, E. L. (1989) *Proc. Natl. Acad. Sci. USA* **86,** 5773–5777.
13. Janmey, P. A., Cunningham, C. C., Oster, G. F. & Stossel, T. P. (1992) in *Mechanics of Swelling. From Clays to Living Cells and Tissues,* ed. Karalis, T. K. (Springer, Berlin), pp. 333–346.
14. Bärmann, M., Käs, J., Kurzmeier, H. & Sackmann, E. (1992) in *The Structure and Conformation of Amphiphilic Membranes.* Springer Proceedings in Physics Vol. 66, eds. Lipowsky, R., Richter, D. & Kremer, K. (Springer, Berlin), pp. 137–143.
15. Grimm, R., Bärmann, M., Häckl, W., Typke, D. Sackmann, E. & Baumeister, W. (1997) *Biophys. J.* **72,** 482–489.
16. Häckl, W., Bärmann, M. & Sackmann, E. (1998) *Phys. Rev. Lett.* **80,** 1786–1789.
17. Miyata, H. & Hotani, H. (1992) *Proc. Natl. Acad. Sci. USA* **89,** 11547–11551.
18. Hotani, H. & Miyamoto, H. (1990) *Adv. Biophys.* **26,** 135–156.
19. Isambert, H., Venier, P., Maggs, A. C., Fattoum, A., Kassab, R., Pantaloni, D. & Carlier, M.-F. (1995) *J. Biol. Chem.* **270,** 11437–11444.
20. Venier, P., Maggs, A. C., Carlier, M.-F. & Pantaloni, D. (1994) *J. Biol. Chem.* **269,** 13353–13360.
21. Small, J. V., Rottner, K., Kaverina, I. & Anderson, K. I. (1998) *Biochim. Biophys. Acta* **1404,** 271–281.
22. Spudich, J. A. & Watt, S. (1971) *J. Biol. Chem.* **246,** 4866–4871.
23. MacLean-Fletcher, S. & Pollard, T. D. (1980) *Biochem. Biophys. Res. Commun.* **96,** 18–27.
24. Knight, P. & Offer, G. (1978) *Biochem. J.* **175,** 1023–1032.
25. Akashi, K.-i., Miyata, H., Itoh. H. & Kinosita, K., Jr. (1996) *Biophys. J.* **71,** 3242–3250.
26. Hibino, M., Shigemori, M., Itoh, H., Nagayama, K. & Kinosita, K., Jr. (1991) *Biophys. J.* **59,** 209–220.
27. Tzong, T. Y. (1991) *Biophys. J.* **60,** 297–306.
28. Jezek, P., Mahdi, F. & Garlid, K. D. (1990) *J. Biol. Chem.* **265,** 10522–10526.
29. Kinosita, K. Jr., Hibino, M., Itoh, H., Shigemori, M., Hirano, K., Kirino, Y. & Hayakawa, T. (1992) in *Guide to Electroporation and Electrofusion,* eds. Chang, D. C., Chassy, B. M., Saunders, J. A. & Sowers, A. E. (Academic, New York), pp. 29–46.
30. Schmidt, C. F., Bärmann, M., Isenberg, G. & Sackmann, E. (1989) *Macromolecules* **22,** 3638–3649.
31. Hyuga, H., Kinosita, K., Jr. & Wakabayashi, N. (1991) *Jpn. J. Appl. Phys.* **30,** 1141–1148.
32. Deuling, H. J. & Helfrich, W. (1976) *J. Physique* **37,** 1335–1345.
33. Hochmuth, R. M., Mohandas, N. & Blackshear, P. L., Jr. (1973) *Biophys. J.* **13,** 747–762.
34. Hotani, H. (1984) *J. Mol. Biol.* **178,** 113–120.
35. Servuss, R. M., Harbich, W. & Helfrich, W. (1976) *Biochim. Biophys. Acta.* **436,** 900–903.
36. Furukawa, R. Kundra, R. & Fechheimer, M. (1993) *Biochemistry* **32,** 12346–12352.
37. Wessels, D., Vawter-Hugart, H., Murray, J. & Soll, D. R. (1994) *Cell Motil. Cytoskeleton* **27,** 1–12.
38. Zigmond, S. H. (1993) *Cell Motil. Cytoskeleton* **25,** 309–316.
39. Bretcher, A. & Weber. K. (1980) *Cell* **20,** 839–847.
40. Mullins, R. D., Heuser, J. A. & Pollard, T. D. (1998) *Proc. Natl. Acad. Sci. USA* **95,** 6181–6186.
41. Welch, M. D., Rosenblatt, J., Skoble, J., Portnoy, D. A. & Mitchison, T. J. (1998) *Science* **281,** 105–108.
42. Chan, A. Y., Raft, S., Bailly, M., Wyckoff, J. B., Segall, J. E. & Condeelis, J. S. (1998) *J. Cell Sci.* **111,** 199–211.